

High-temperature deep-level transient spectroscopy system for defect studies in wide-bandgap semiconductors

Cite as: Rev. Sci. Instrum. 90, 063903 (2019); doi: 10.1063/1.5097755

Submitted: 28 March 2019 • Accepted: 30 May 2019 •

Published Online: 20 June 2019



S. Majdi,^{1,a)} M. Gabrysch,¹ N. Suntornwipat,¹ F. Burmeister,¹ R. Jonsson,¹ K. K. Kovi,^{1,2} and A. Hallén^{3,4}

AFFILIATIONS

¹Department of Engineering Sciences, Division of Electricity, Uppsala University, Box 534, 751 21 Uppsala, Sweden

²Center for Nanoscale Materials, Argonne National Laboratory, Argonne, Illinois 60439, USA

³Royal Institute of Technology, KTH-ICT, Electrum 229, 164 40 Stockholm, Sweden

⁴Department of Physics and Astronomy, Ion Physics, Uppsala University, Box 516, 751 20 Uppsala, Sweden

^{a)}Author to whom correspondence should be addressed: Saman.Majdi@angstrom.uu.se. Tel.: +46 (0) 18 471 5854.

Fax: +46 (0) 18 471 5810.

ABSTRACT

Full investigation of deep defect states and impurities in wide-bandgap materials by employing commercial transient capacitance spectroscopy is a challenge, demanding very high temperatures. Therefore, a high-temperature deep-level transient spectroscopy (HT-DLTS) system was developed for measurements up to 1100 K. The upper limit of the temperature range allows for the study of deep defects and trap centers in the bandgap, deeper than previously reported by DLTS characterization in any material. Performance of the system was tested by carrying out measurements on the well-known intrinsic defects in *n*-type 4H-SiC in the temperature range 300–950 K. Experimental observations performed on 4H-SiC Schottky diodes were in good agreement with the literature. However, the DLTS measurements were restricted by the operation and quality of the electrodes.

Published under license by AIP Publishing. <https://doi.org/10.1063/1.5097755>

INTRODUCTION

Substitution of chemically different impurity atoms into a host semiconductor can generate deep-level states in the bandgap. Additionally, substantial variation from the ordered lattice, for instance a vacant lattice position, can give rise to allowed states between the conduction and valence band close to the midgap. Such centers are not always ionized at room-temperature. Deep states act as efficient electron-hole recombination centers that reduce carrier lifetimes, particularly in indirect semiconductors. In some instances, deep-levels are deliberately introduced to increase switching speed for semiconductor devices by reducing the minority carrier lifetime, e.g., in fast switching power devices.

Deep-level transient spectroscopy (DLTS) is a powerful electrical characterization method based on measuring the depletion region capacitance of a Schottky or *pn*-junction.^{1–4} If there are deep-levels present, this capacitance will change as a function of time due

to the emission of trapped carriers.⁵ It is complementary to other methods for identifying defects, e.g., photoluminescence, electron spin resonance and isothermal capacitance transient spectroscopy (ICTS), which is equivalent to DLTS measurements but is done in a time domain under constant temperature.⁶ DLTS, however, being an all-electric method, gives information about electrically active defects and impurities and is a highly sensitive technique, capable of detecting and quantifying very low defect concentrations.^{2,7}

Power electronics based on low-loss semiconductor devices are expected to play a leading role in the development of future power generation, transmission, and distribution systems. Wide-bandgap (WBG) semiconductor materials, such as SiC, GaN, Ga₂O₃, and diamond are considered to be extremely promising. SiC is the most mature WBG material which has been frequently investigated using DLTS during decades, but still reveals defect-related findings.⁸ Ga₂O₃ is another interesting material which recently has attracted great attention.^{9,10} In the case of diamond, the excellent material

working temperatures, and chemical inertness of the material. To prevent unnecessary heating of the chamber walls and the mounting stage in the chamber and also to assure even sample heating, a heat shield, consisting of two molybdenum (Mo) shielding boxes and ceramic insulators, was used. Two high-temperature thermocouples (type K) are connected to the ceramic heater and the Ta plate directly under the sample. A Tectra HC3500 controller/power supply based on a Yudian AI 518P PID temperature-controller is used as power source for sample heating.

Multiple electrical characterizations are possible using four Ta probes mounted in an electrically insulating holder, made of the ceramic material, Macor (stable up to 1300 K). Electrical measurements are performed by using a HP/Agilent 4280A 1 MHz (C meter/CV plotter) which can record transient signals needed for extracting high resolution DLTS signals coupled to an HP/Agilent 50 MHz 8112A programmable dual pulse generator. Both are controlled via the general purpose interface bus (GPIB). To suppress the background noise, a low-pass filter has been built. A manual switch box was constructed to enable measurements on different sample configurations. Running and monitoring the experiment is fully automated by LabVIEW software.

The temperature range operation of the DLTS system was investigated by performing a series of heating test using a synthetic diamond sample. The sample was mounted in the ceramic sample holder, heated up to 1100 K in vacuum, and remained in such condition for an hour. This procedure was repeated and successfully carried out with no evidence of degradation on neither the sample nor the parts in the system. The chamber pressure could be kept at a constant level of 5×10^{-6} mbar during the entire measurement after 30 min of prepumping.

EXPERIMENTAL

In the present work, an *n*-type 4H-SiC sample was prepared and analyzed for testing and calibration of the setup. The 4H-SiC Schottky diodes were manufactured from *n*-type substrate wafers with a 10 μm thick *n*-type epitaxial layer purchased from Cree. The Schottky barrier is provided by circular Ni (150 nm thick) contacts

with a diameter of 250 and 500 μm respectively, produced by electron beam evaporation. 200 nm Al was deposited on the backside of the sample forming an Ohmic contact to the highly doped substrate.

To ensure good rectification, the Schottky diodes were characterized by current-voltage (IV) and capacitance-voltage (CV) measurements determining the doping concentrations and overall functionality. The CV measurements were performed from room-temperature up to the breakdown point of the electrodes at 950 K (see Fig. 3). Typical net doping concentrations, $N_d - N_a$, determined from the slope when plotting $1/C^2$ vs reverse voltage, were in the range of $2 \times 10^{15} \text{ cm}^{-3}$ at room-temperature.

To observe the intrinsic deep-levels in *n*-type 4H-SiC, HT-DLTS was performed in the temperature range 300–950 K. The following DLTS parameters were used: a filling pulse of 50 ms width and 10 V height in addition to the constant reverse bias $V_r = -10 \text{ V}$. To evaluate the capacitance transient, the conventional lock-in amplification was used to reduce the noise level and to achieve a high signal-to-noise ratio. The DLTS signal is obtained by pulsing the applied bias and observing a transient decay of trapped charge carriers in the depletion region. The analysis of the capacitance transients follows a scheme outlined in (Ref. 21), where arbitrary wave functions can be used for the evaluation.

RESULTS AND DISCUSSIONS

DLTS studies are highly sensitive measurements, retaining certain demands on the samples. The maximum concentration of defects should preferably not exceed 10% of the doping density²² to enable reliable quantitative analysis. For WBG materials, very high temperatures are needed to access the entire bandgap. The capacitance transient is studied as a function of temperature and, after signal processing, one obtains the DLTS spectrum. An electrically active deep-level appears in the spectrum as a peak for a certain temperature and measurement frequency. The peak height is proportional to the (uniform) trap concentration. Analyzing the peak positions provides information about the energy position in the bandgap and the carrier capture cross section. As mentioned

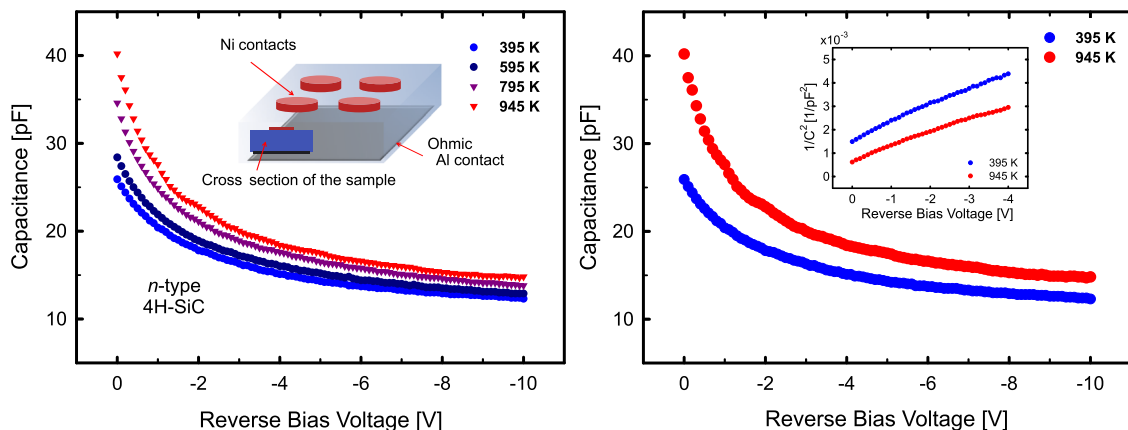


FIG. 3. Capacitance-voltage sweep of the reverse biased junction in *n*-type 4H-SiC, measured at different temperatures. The insets describe (left) the schematic of the diode and (right) $1/C^2$ characteristic of the 4H-SiC sample.

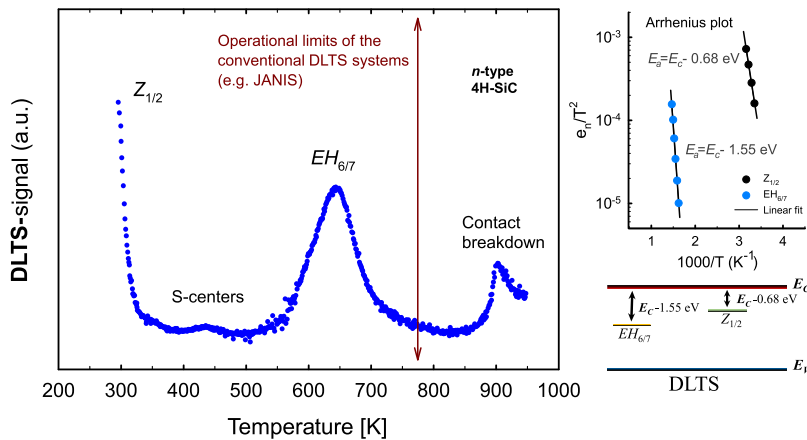


FIG. 4. HT-DLTS spectrum (left) measured with a period width of 50 ms in the temperature range from 300 to 950 K obtained from *n*-typed 4H-SiC Schottky structure. The Arrhenius plot (right) gives the related position of the defects in the bandgap.

before, the analytic method used in our experiment is based on the conventional lock-in principle.²¹

In high-quality *n*-type 4H-SiC epilayers, two deep-levels are often seen in DLTS positioned at 0.56–0.71 eV and 1.55–1.65 eV below the conduction band edge. It has been shown that these levels originate from different charge states of the carbon vacancy.⁸ The more shallow state, $Z_{1/2}$, is a double acceptor level, where the first transition ($-2|-1$) is very fast and normally only the second transition is seen in DLTS ($-1|0$). The deeper state is named $EH_{6/7}$, but it is only EH_7 of this complex that belongs to the carbon vacancy and the donor transition ($0|+1$).

Here, the DLTS peaks of the $Z_{1/2}$ and the $EH_{6/7}$ transitions can clearly be observed for our sample measured on a Schottky structure (see Fig. 4.). The activation energies are found by measuring a set of emission rates (e_n) as function of temperature and plotting $\ln(e_n/T^2)$ vs $1/T$, often referred to as an Arrhenius plot. The results achieved from the slope of the Arrhenius plot revealed full agreement with the data in the literature, 0.68 eV and 1.55 eV below the conduction band for $Z_{1/2}$ and $EH_{6/7}$ state, respectively.

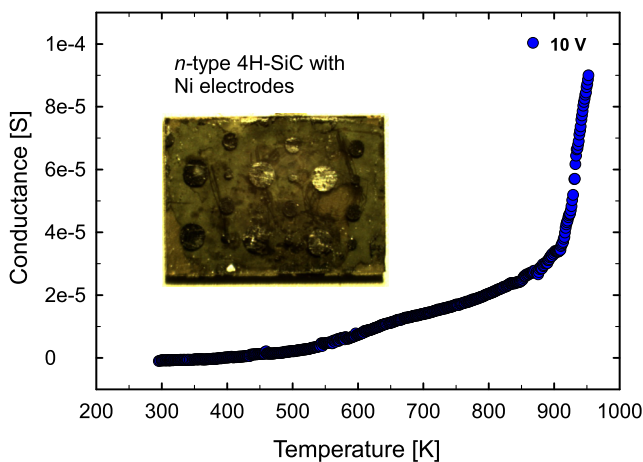


FIG. 5. The change of the conductance in *n*-type 4H-SiC sample is recorded as function of temperature at 10 V applied bias.

Having a low pressure is important to extend the lifetime of the electrodes and to increase the operational limit of the Schottky diodes up to higher temperatures. In DLTS measurements, it is crucial for detection of small changes in the capacitance to achieve a stable rectification. The capacitance transient is highly sensitive to fluctuations of the conductivity. Hence, when the conductivity increases at elevated temperatures due to the excess of higher thermionic energy, the emission process becomes much faster which reduces the rectification, increases the leakage current and conductance, and finally results in breakdown of the electrodes. In Fig. 5, one can see how the conductivity at a certain point rapidly increases and reaches a critical level. From this point, it is no longer possible to detect a DLTS signal. This is most likely due to the degradation and finally failure of the Ni contacts' Schottky properties. According to earlier studies, at temperatures around 600 °C, Ni₂Si phase formation appears at the Ni/SiC interface. The transition from Schottky to Ohmic contact in a nickel silicide/SiC system during annealing is a well-known phenomenon.^{23,24} In case of diamond however, studies show that the Schottky operation of diodes can be extended to higher temperatures by careful selection of contact material, e.g., ruthenium and copper.^{25,26}

CONCLUSIONS

In summary, we have developed a high-temperature deep-level transient spectroscopy system for investigating deep defects in WBG semiconductor materials. Many of the important features of the defects and trap centers in such materials have not been identified so far. A reason is the lack of suitable electrical and high-temperature stable environment in conventional DLTS setups. However, with the higher temperature range of this system, it is now possible to explore the bandgap of semiconductors much deeper than before.

Here, we provide experimental evidence by using an *n*-type 4H-SiC sample for calibration and to determine the function of the built setup. DLTS measurements were successfully performed up to 950 K where the well-known defect complex $EH_{6/7}$ could be observed and the energy position in the bandgap extracted.

However, the DLTS measurements could not reach up to the temperature limit of the system at 1100 K due to the failure of the Schottky contacts. Hence, achieving high quality diodes with good

rectifying characteristics for operation at elevated temperatures is extremely important to fully use the potential of the system.

ACKNOWLEDGMENTS

The Carl Trygger Foundation (13:284), LM Ericsson Research Foundation, and Magnus Bergvalls Foundation are gratefully acknowledged for financial support.

REFERENCES

- ¹P. Blood and J. W. Orton, *Electrical Characterization of Semiconductors: Majority Carriers Properties* (Academic Press, London, 1992).
- ²D. V. Lang, *J. Appl. Phys.* **45**, 3023 (1974).
- ³G. L. Miller, D. V. Lang, and L. C. Kimerling, *Annu. Rev. Mater. Sci.* **7**, 377 (1977).
- ⁴D. Pons, *J. Appl. Phys.* **55**, 3644 (1984).
- ⁵L. Dobaczewski, A. R. Peaker, and K. Bonde Nielsen, *J. Appl. Phys.* **96**, 4689 (2004).
- ⁶H. Okushi and Y. Tokumaru, *Jpn. J. Appl. Phys., Part 2* **19**, L335 (1980).
- ⁷A. R. Peaker, V. P. Markevich, and J. Coutinho, *J. Appl. Phys.* **123**, 161559 (2018).
- ⁸N. T. Son, X. T. Trinh, L. S. Løvlie, B. G. Svensson, K. Kawahara, J. Suda, T. Kimoto, T. Umeda, J. Isoya, T. Makino, T. Ohshima, and E. Janzén, *Phys. Rev. Lett.* **109**, 187603 (2012).
- ⁹S. J. Pearton, J. Yang, P. H. Cary, F. Ren, J. Kim, M. J. Tadjer, and M. A. Mastro, *Appl. Phys. Rev.* **5**, 011301 (2018).
- ¹⁰M. Higashiwaki and G. H. Jessen, *Appl. Phys. Lett.* **112**, 060401 (2018).
- ¹¹S. Majdi, K. K. Kovi, J. Hammersberg, and J. Isberg, *Appl. Phys. Lett.* **102**, 152113 (2013).
- ¹²M. Gabrysch, S. Majdi, D. J. Twitchen, and J. Isberg, *J. Appl. Phys.* **109**, 063719 (2011).
- ¹³S. Majdi, M. Gabrysch, K. K. Kovi, N. Suntornwipat, I. Friel, and J. Isberg, *Appl. Phys. Lett.* **109**, 162106 (2016).
- ¹⁴T. P. Chow, I. Omura, M. Higashiwaki, H. Kwarada, and V. Pala, *IEEE Trans. Electron Devices* **64**, 856 (2017).
- ¹⁵S. Koizumi, H. Umezawa, J. Pernot, and M. Suzuki, *Power Electronics Device Applications of Diamond Semiconductors*, 1st ed. (Woodhead Publishing, 2018).
- ¹⁶G. Balasubramanian, P. Neumann, D. Twitchen, M. Markham, R. Kolesov, N. Mizuochi, J. Isoya, J. Achard, J. Beck, and J. Tessler, *Nat. Mater.* **8**, 383 (2009).
- ¹⁷N. Mizuochi, T. Makino, H. Kato, D. Takeuchi, M. Ogura, H. Okushi, M. Nothaft, P. Neumann, A. Gali, F. Jelezko, J. Wrachtrup, and S. Yamasaki, *Nat. Photonics* **6**, 299 (2012).
- ¹⁸J. P. Goss, P. R. Briddon, and M. J. Shaw, *Phys. Rev. B* **76**, 075204 (2007).
- ¹⁹F. M. Hrubesch, G. Braunbeck, M. Stutzmann, F. Reinhard, and M. S. Brandt, *Phys. Rev. Lett.* **118**, 037601 (2017).
- ²⁰A. M. Edmonds, U. F. S. D'Haenens-Johansson, R. J. Cruddace, M. E. Newton, K.-M. C. Fu, C. Santori, R. G. Beausoleil, D. J. Twitchen, and M. L. Markham, *Phys. Rev. B* **86**, 035201 (2012).
- ²¹B. G. Svensson, K.-H. Rydén, and B. M. S. Lewerentz, *J. Appl. Phys.* **66**, 1699 (1989).
- ²²W. M. Vetter, J. Q. Liu, M. Dudley, M. Skowronski, H. Lendenmann, and C. Hallin, *Mater. Sci. Eng.: B* **98**, 220 (2003).
- ²³S. Y. Han, K. H. Kim, J. K. Kim, H. W. Jang, K. H. Lee, N.-K. Kim, E. D. Kim, and J.-L. Lee, *Appl. Phys. Lett.* **79**, 1816 (2001).
- ²⁴J. Crofton, P. G. McMullin, J. R. Williams, and M. J. Bozack, *J. Appl. Phys.* **77**, 1317 (1995).
- ²⁵K. Ikeda, H. Umezawa, K. Ramanujam, and S. Shikata, *Appl. Phys. Express* **2**, 011202 (2009).
- ²⁶K. Ueda, K. Kawamoto, and H. Asano, *Diamond Relat. Mater.* **57**, 28 (2015).